Heterogeneous Reactions of Methylglyoxal in Acidic Media: Implications for Secondary Organic Aerosol Formation

JUN ZHAO,[†] NICHOLAS P. LEVITT,[†] RENYI ZHANG,*,[†] AND JIANMIN CHEN[‡]

Department of Atmospheric Sciences, Texas A&M University, College Station, Texas 77843, and Department of Environmental Science & Engineering, Fudan University, Shanghai 200433, P. R. China

Recent environmental chamber studies have suggested that acid-catalyzed particle-phase reactions of organic carbonyls contribute to the formation of secondary organic aerosol (SOA). We report the first measurements of uptake of methylglyoxal on liquid H_2SO_4 over the temperature range of 250–298 K and acidic range of 55–85 wt %. From the time-dependent uptake the effective Henry's law solubility constant (H^*) was determined. Heterogeneous reactions of methylglyoxal are shown to decrease with acidity and involve negligible formation of sulfate esters. Hydration and polymerization likely explain the measured uptake of methylglyoxal on H_2SO_4 and the measurements do not support an acid-catalyzed uptake of methylglyoxal. The results imply that heterogeneous reactions of methylglyoxal contribute to organic aerosol formation in less acidic media and hydration and polymerization of methylglyoxal in the atmospheric aerosol-phase are dependent on the hygroscopicity, rather than the acidity of the aerosols.

Introduction

In acidic media carbonyl (aldehyde and ketone) compounds engage in aqueous-phase reactions, such as hydration, polymerization, hemiacetal/acetal formation, aldol condensation, or cationic rearrangement (*1, 2*). Recent interest in this area has arisen from the intermediacy of these compounds in heterogeneous or acid-catalyzed reactions which contribute to the formation of secondary organic aerosols (SOA) in the atmosphere (*3, 4*). On the basis of environmental chamber measurements, reactions of carbonyls in the aerosol-phase have been suggested to result in formation of low-vapor pressure products or polymers, which considerably increases the amount of organic mass produced. SOA formation has major impacts in the atmosphere, including visibility reduction, cloud formation, direct and indirect radiative forcing, and adverse health effects (*5, 6*).

One such a carbonyl reaction involves methylglyoxal (CH_3-COCHO) produced in the atmosphere from photochemical oxidation of volatile organic compounds (VOCs). Oxidation of anthropogenic aromatics (toluene, xylenes, or trimethylbenzenes) and biogenic isoprene leads to significant production of methylglyoxal in the urban and regional
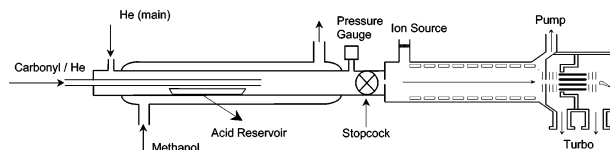
* Corresponding author phone: 979–845-7656; fax: 979–862-4466; email: zhang@ariel.met.tamu.edu.
  † Texas A&M University.
  ‡ Fudan University.

FIGURE 1. Schematic representation of the flow reactor coupled to the ID–CIMS.

atmospheres (*7–9*). For example, the molar molecular yield of methylglyoxal is about 0.9 from 1,3,5-trimethylbenzene oxidation and 0.16 for toluene oxidation (*4*). Concentrations of methylglyoxal up to ppb (parts per billion) levels have been measured in polluted air (*10*). In the gas-phase, photolysis or reaction with the OH radical has been identified as the major loss process for methylglyoxal, with the corresponding lifetimes of 1–3 h for solar zenith angles of 0–60° and 23 h for an average OH concentration of 10^6 molecules cm^{-3} (*11*). In general, the SOA yields are high with less methyl substituted aromatics when comparing toluene to 1,3,5-trimethylbenzene. Toluene and mono-alkyl benzene are categorized as a group of high aerosol production in the aromatic system, and a strong nonlinear relationship was observed between measured SOA yields and production of unsaturated dicarbonyl aldehydes resulting from ring-fragmenting of aromatics (*7–9*). However, in the environmental chamber experiments of photooxidation of 1,3,5-trimethylbenzene, significant polymerization reactions were observed to take place in aerosols and were attributed to hydration and subsequent reactions of methylglyoxal along with other carbonyl products (*4*). The chemical mechanism of the interaction of methylglyoxal with atmospheric aerosols, however, remains poorly understood, hindering development of predictive models to assess its role in SOA formation.

We report in this work heterogeneous chemistry of methylglyoxal with liquid H_2SO_4 over the temperature range of 250–298 K and acidic range of 55–85 wt %. Uptake of methylglyoxal on liquid sulfuric acid was studied using a fast-flow reactor coupled to ion drift–chemical ionization mass spectrometry (ID–CIMS). From the time-dependent uptake the effective Henry's law solubility constant (H^*) was determined. Implications of the present results on SOA formation are discussed.

Experimental Section

The experiments were carried out in a flow reactor coupled to an ion drift–chemical ionization mass spectrometer (ID–CIMS) as shown in Figure 1, similarly to our previous work (*12*). Briefly, the Pyrex reactor was 50 cm long and with an internal radius of 1.25 cm. Liquid H_2SO_4 was placed within an inner Pyrex vessel, which was recessed to form a trough (2.0 cm wide and 0.7 cm deep) to hold the liquid solution. The geometric area of sulfuric acid was calculated from the dimension of the Pyrex vessel, which was about 40 cm^2. The temperature of the flow reactor was controlled by flowing cold methanol through the outer jacket of the reactor and was measured by a thermocouple. All carrier flows were monitored with calibrated electronic mass flow meters (Millipore Tylan 260 Series). The flow reactor was operated under the laminar flow conditions with a pressure of about 1 Torr and flow velocities of 800–1000 cm s^{-1}. Typical flow rate was 0.30–0.35 slpm (liter per minute at standard temperature and pressure). Helium was used as the main carrier gas. H_2SO_4 solutions were prepared by dilution of 96 wt % H_2SO_4 with distilled water. The acid reservoir was changed and the composition of the acid was checked before
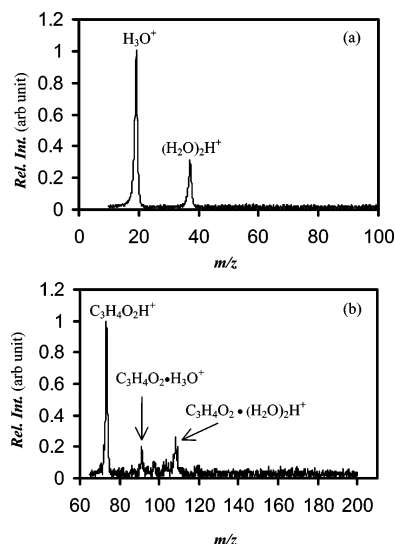
FIGURE 2. Spectral scans for the reagent ions (a, $m/z = 10\sim100$) and protonated methylgloxal (b, $m/z = 60\sim200$) for a typical experimental condition (before an uptake experiment).

and after each experiment. The acid compositions were verified by density measurements and by titration with standardized NaOH. During the experiment, water vapor was added to the flow reactor to reduce H_2O evaporation from the liquid and to minimize changes in the acid composition (13, 14). H_2O partial pressure could not be monitored by ID−CIMS.

Commercially available methylglyoxal as a 40% aqueous solution (Aldrich) existed primarily in its monohydrate and dihydrate forms. To obtain the unpolymerized and water-free form, the following procedure was used: ca. 20 mL of methylglyoxal aqueous solution was pumped under vacuum overnight in a flask covered with a black cloth in order to remove water and to prevent slow decomposition by room light (15). The resulting highly viscous and dark liquid was rapidly heated up to at least 180 °C until only a black and crispy residue remained. The distillate passed subsequently through columns containing anhydrous calcium sulfate ($CaSO_4$) and phosphorus pentoxide (P_2O_5) and was collected in a dry ice trap (~ -78 °C). Freshly prepared methylglyoxal (green-yellowish liquid) was pumped at the temperature of dry ice for at least 30 min before use to remove impurities such as CO, H_2CO, and acetic acid from the sample. Purity of methylglyoxal was checked by the mass spectrometry before an uptake experiment. The saturation vapor pressure (P^0) of methylglyoxal was determined by (16, 17)

$$\ln\left(\frac{P^0}{760}\right) = \frac{\Delta S_{vap}(T_b)}{R}\left[1.8\left(1 - \frac{T_b}{T}\right) + 0.8\ln\left(\frac{T_b}{T}\right)\right] \text{ (torr)} \tag{1}$$

where R is the molar gas constant (8.314 J mol^{-1} K^{-1}), ΔS_{vap} is the entropy of vaporization (in J mol^{-1} K^{-1}), T_b is the boiling point and T is the temperature of the dry ice−acetone bath for the methylglyoxal bubbler (in K). ΔS_{vap} was calculated using a modified Trouton's method (18, 19) and boiling points T_b were taken from the literature values (20). Methylglyoxal vapor was introduced into the flow reactor by a movable injector and its partial pressure in the flow reactor was estimated on the order of 10^{-6} to 10^{-7} Torr on the basis of the calculated vapor pressure.

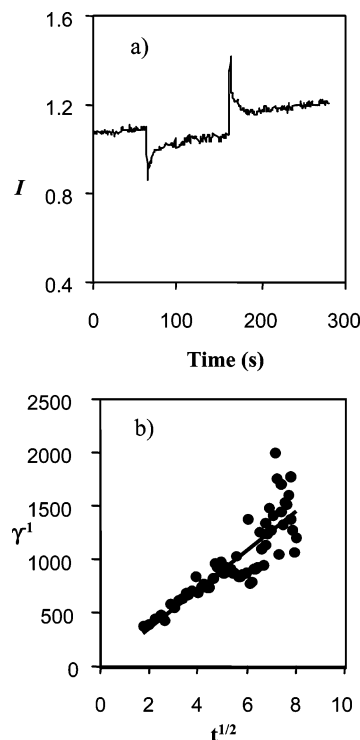Methylglyoxal was detected using ID−CIMS (21, 22), according to the proton-transfer reaction with H_3O^+

$$H_3O^+ + CH_3COCHO \rightarrow CH_3COCHOH^+ + H_2O \tag{2}$$

FIGURE 3. Temporal profiles (I, intensity) of methylgloxal when exposed to a 20 cm length of a vessel containing a 80 wt % H_2SO_4 at $T = 273$ K (a). (b) corresponds to a plots of 1/g vs t $^{1/2}$ corresponding to (a). A steady methylgloxal signal was first established prior to each experiment. Methylgloxal was exposed to H_2SO_4 at about 60 s by pulling the movable injector upstream. The exposure was terminated at 170 s by pushing the injector back to its original position. There was a slightly increasing trend for the baseline in the methylgloxal signal.

where $CH_3COCHOH^+$ denotes protonated methylglyoxal. Methylglyoxal was monitored at its protonated peaks ($m/z = 73$). Figure 2 depicts mass spectra of the reagent ions and the methylglyoxal sample, showing the dominant $CH_3COCHOH^+$ peak along with trace protonated mono- and dihydrates ($C_3H_4O_2\cdot H_3O^+$, $C_3H_4O_2\cdot(H_2O)_2H^+$) ($m/z = 91$ and 109 respectively).

From the measured uptake of methylglyoxal on sulfuric acid, we determined the uptake coefficient and Henry's Law constant. The uptake coefficient was calculated from the initial and time-dependent signals of methylglyoxal (23−25)

$$\gamma(t) = \frac{4k}{\omega}\left(\frac{V}{A}\right) \tag{3}$$

where V is the volume of the flow reactor, A is the geometric area of the exposed acid, ω is the mean thermal speed of the molecule, and k is the first-order rate coefficient related to the fractional change in the gas-phase concentration of methylglyoxal molecule before and after exposure to sulfuric acid. The time-dependent uptake coefficient is also expressed as the following (24):

$$1/\gamma(t) = a + bt^{1/2} \tag{4}$$

where a is a constant related to the accommodation coefficient and time-independent aqueous reaction rate constant and $b = \omega/4H^*RT(D_l/\pi)^{1/2}$. H^* is the effective Henry's law solubility constant, D_l is the liquid-phase diffusion coefficient, R is the gas constant, and T is the temperature. Hence the time-dependent uptake coefficient permits an estimate of the effective Henry's Law Constant. D_l was
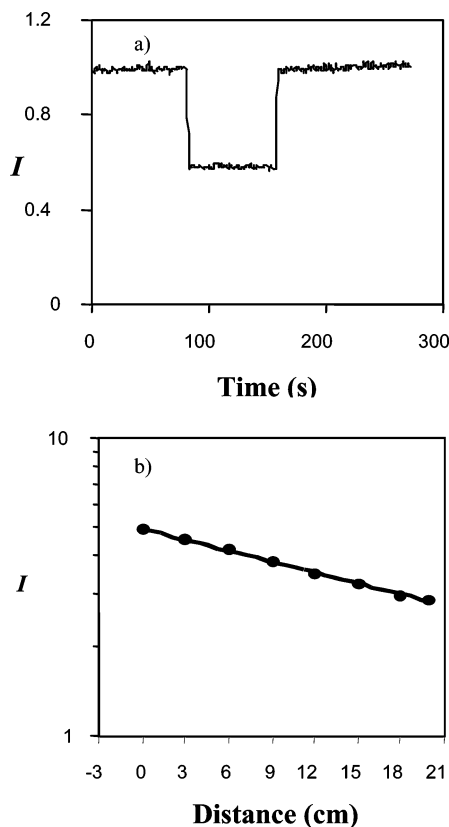
FIGURE 4. Temporal profiles (*I*, relative intensity) of methylgloxal when exposed to a 20 cm length of a vessel containing a 58 wt % H_2SO_4 at $T = 253$ K (a). (b) corresponds to loss of methylglyoxal signals as a function of injector position for similar experimental conditions in (a). Methylgloxal was exposed to H_2SO_4 at about 70 s and the exposure was terminated at 150 s.

estimated according to the method discussed by Klassen et al. (*26*).

Results and Discussion

Uptake of methylglyoxal on H_2SO_4 exhibited distinct patterns, depending on the acidity and temperature. The concentration of methylglyoxal in the gas-phase dropped considerably upon exposure to 80 wt % H_2SO_4 and later returned close to its original value as the H_2SO_4 liquid was saturated (Figure 3). Terminating the methylglyoxal exposure resulted in an opposite peak due to desorption. The shapes of adsorption and desorption were nearly identical, suggesting that methylglyoxal was primarily taken up reversibly, although some methylglyoxal appeared to remain in the solution due to a small irreversible uptake. In contrast, loss of methylglyoxal on H_2SO_4 was more pronounced on 58 wt % H_2SO_4 (Figure 4). The uptake showed little saturation on the time scale of the experiment, indicating an irreversible chemical loss. The uptake on 68 wt % H_2SO_4 exhibited an intermediate behavior compared to those on 80 and 58 wt % H_2SO_4, consisting of noticeable reversible and irreversible components (Figure 5).

The time-dependent uptake coefficients were calculated from the initial and time-dependent methylglyoxal signals. Plots of the inverse uptake coefficient against the square root of time are shown in Figures 3b and 5b. The line fitted to the data in Figure 3b extrapolated closely to the origin, consistent with reversible uptake under high acidity. Extrapolation of the fitting line in Figure 5b showed an offset from the origin, because of a reactive loss. The effective Henry law's constant (H^*) was determined from the slope of the linear least-square fit of the data (eq 4) and summarized in
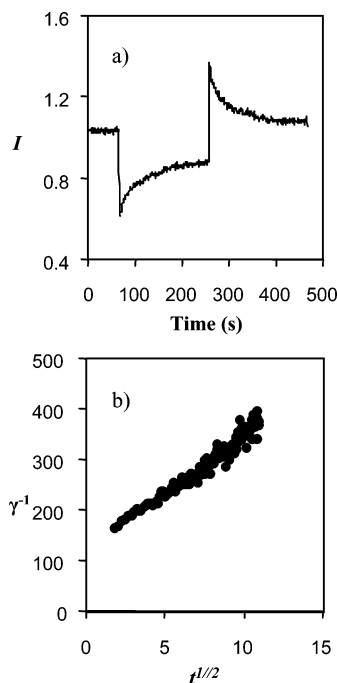

FIGURE 5. Temporal profiles (*I*, relative intensity) of methylglyoxal when exposed to a 20 cm length of a vessel containing a 68 wt % H_2SO_4 at $T = 263$ K. (b) plots $1/\gamma$ vs t $^{1/2}$ corresponding to data in (a). Methylgloxal was exposed to H_2SO_4 at about 70 s and the exposure was terminated at about 250 s.

TABLE 1. Summary of H^* for Methylglyoxal in H_2SO_4[a]

T (K)	H_2SO_4 (wt %)	$H^*(\times 10^3$ M atm^{-1})
253	79	55.5 ± 13.7
263	68	33.6 ± 6.4
263	79	21.2 ± 6.5
273	64	24.9 ± 2.0
273	69	15.2 ± 3.2
273	80	6.7 ± 1.6
283	73	5.9 ± 0.1
283	80	4.0 ± 0.9
296	81	2.6 ± 0.2

[a] Each point averages over at least three measurements.

Table 1. The measured H^* depended on both temperature and acidity, increasing with decreasing temperature and decreasing acidity. The H^* value increased from 6.7×10^3 to 25×10^3 M atm^{-1} for 80−64 wt % H_2SO_4 at 273 K, while for 68−69 wt % H_2SO_4 H^* increased from 15×10^3 to 34×10^3 M atm^{-1} from 273 to 263 K. The H^* value of 2600 M atm^{-1} for 81 wt % H_2SO_4 at room temperature was smaller than that of 3700 M atm^{-1} previously reported for methylglyoxal in pure water solution (*27*). For the irreversible uptake, the decay of the methylglyoxal signal followed pseudo-first-order kinetics; a time-independent uptake coefficient of 7.6×10^{-3} was obtained from Figure 4b. A recent study of reactive uptake of glyoxal on acidic aerosols reported uptake coefficients of 8.0×10^{-4} to 7.3×10^{-3} at room temperature (*28*).

For a given temperature, the uptake of methylglyoxal on H_2SO_4 decreased with acidity, indicating a dependence on water activity. This implies that aqueous reactions of methylglyoxal in H_2SO_4 are dominant by hydration and subsequent polymerization. The amount of available water in the solution impacts the equilibrium between the free (unhydrated) and hydrated forms of methylglyoxal. In concentrated H_2SO_4, the small water activity hinders hydration and further polymerization reactions, corresponding to a solubility-limited reversible uptake. In dilute H_2SO_4 with
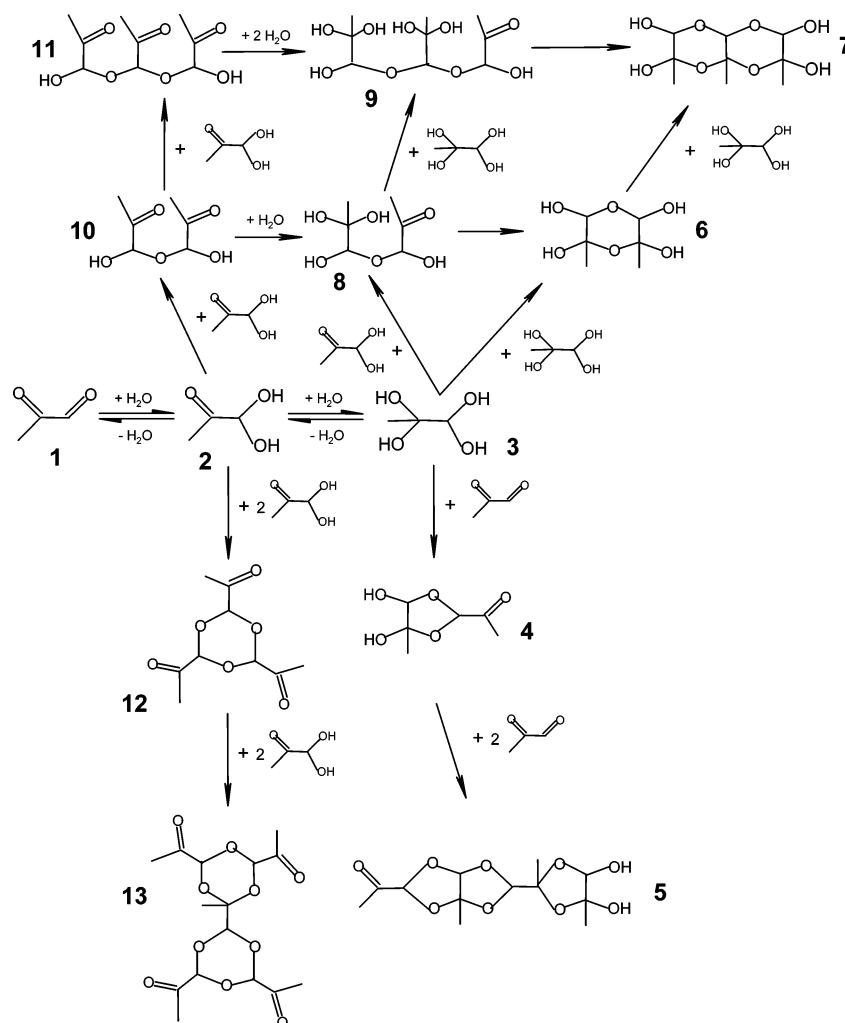
FIGURE 6. Possible aqueous reaction mechanism of methylglyoxal in H_2SO_4.

large water activity, the equilibrium is shifted nearly completely toward the hydrated forms of methylglyoxal, with a negligible reversible reaction. In our experiments, the partial pressure of methylglyoxal was very low (on the order of 10^{-6} to 10^{-7} Torr) so that uptake of methylglyoxal did not change appreciably the water activity in the solution. Subsequent polymerization reactions lead to formation of low-vapor pressure oligomers that remain in the aqueous-phase, explaining the irreversible uptake in dilute H_2SO_4.

Plausible mechanisms of the aqueous reactions of methylglyoxal in H_2SO_4 are depicted in Figure 6, showing hydration reactions and formation of various oligomers. Initial dissolution and hydration of methylglyoxal (1) result in the diol formation (2), and further hydration produces a tetrol (3). These two hydrates have been identified as the major forms in pure water solution, consisting of 56−62% for monohydrate (diol) and 38−44% for dihydrate (tetrol) (29). Acetal polymerization with methylglyoxal as the main monomer unit leads to formation of acetal polymers (4 and 5). Alternatively, self-reactions and cross-reactions between diols and/or tetrols produce other oligomers as shown in Figure 6. Evidence has been provided for the formation of dimers (6, 8, and 10) and cyclic trimer (12) in aqueous methylglyoxal solution (29). The self-reaction of tetrols (3) or diols (2) results in the formation of a cyclic dimer (6) or a noncyclic dimer (10), respectively. The cross-reaction between diols and tetrols leads to the formation of a dimer (8). The formation of a cyclic trioxane (12) is attributable to a termolecular reaction of diols (2). The produced dimers (6, 8, and 10) or a trimer (12) further engage in reactions with

diols or tetrols, yielding higher oligomers (e.g., 7, 9, 11, and 13). In addition, cyclic oligomers 6 and 7 are likely formed from hydration of 10 and 11, followed by cyclization of 8 and 9, respectively.

Polymers were identified as major components in atmospheric organic aerosols from photooxidation of aromatic compounds in the environmental chamber experiments (4). Measurements using laser desorption LDI−MS confirmed the formation of oligomers up to nonamer (i.e., via 3, 4, and 5) in aqueous solution of methylglyoxal; other mass peaks were also identified likely to be formed from polymerization of 5, 7, 9, or 11 (4). For an analogue α-dicarbonyl, acetal polymer structures represent the dominant forms of oligomers in aqueous glyoxal solutions between 1 and 10 M (30).

Esterification of alcohols by sulfuric acid also occurs at room temperature in bulk solution (31−33). A recent study identified the formation of sulfate esters by esterification of hydrated glyoxal on particulate matter (34). The sulfate esterification mechanism was also invoked to explain irreversible uptake of hydrated formaldehyde in aqueous acidic surfaces (34). We did not observe an irreversible uptake of methylglyoxal in concentrated H_2SO_4, suggesting that the reactions of the hydrated methylglyoxal or oligomers containing the alcohol functional group with sulfuric acid was negligible compared to hydration and polymerization.

The uptake of methylglyoxal in H_2SO_4 was distinct from those of larger aldehydes. For example, the interaction of octanal and 2,4-hexadienal with H_2SO_4 has been explained by aldol condensation that increases with acidity (12). While with negligible hydration rates, octanal, 2,4-hexadienal, and

other high molecular weight carbonyl compounds undergo primarily protonation and enolization, which are then followed by aldol condensation and formation of large unsaturated polymers in high acidity. In contrast, the smaller α-dicarbonyls (e.g., glyoxal and methylgloxal) generally correspond to large hydration rates, leading to aqueous reactions such as hydration, polymerization, even in the absence of an acidic media. The heterogeneous reactions of α-dicarbonyls in acidic aerosols were proposed to be acid-catalyzed (3). We found little evidence for acid-catalyzed reactions of methylglyoxal, since in concentrated H_2SO_4 (high H^+ concentrations) the uptake decreased dramatically with the acidity.

In a recent experimental study of reactive uptake of simple carbonyl species using the laboratory chamber, no growth was observed for most carbonyls including methylglyoxal on aqueous seed particle consisting of ammonium sulfate or mixed ammonium sulfate/sulfuric acid (36). The discrepancy in the methylglyoxal uptake on acidic solutions between the present experiments using the low-pressure fast flow reactor and the previous environmental chamber study remains to be resolved in future studies.

Conclusions

In the present work, we have investigated the heterogeneous chemistry of methylglyoxal with liquid H_2SO_4 over the temperature range of 250–298 K and acidic range of 55–85 wt %, using a fast-flow reactor coupled to ion drift–chemical ionization mass spectrometry (ID–CIMS). This technique permits direct assessment of the heterogeneous interaction between methylglyoxal and H_2SO_4. We have reported the first measurements of heterogeneous uptake of methylglyoxal on liquid H_2SO_4. From the time-dependent uptake the effective Henry's law solubility constant (H^*) was determined. Uptake of methylglyoxal on sulfuric acid decreases with acidity. Hydration and polymerization likely explain our measured uptake of methylglyoxal in H_2SO_4. The measurements did not show an acid-catalyzed uptake of methylglyoxal and revealed negligible sulfate esterification of methylglyoxal in H_2SO_4. Our results suggest that heterogeneous reactions of methylglyoxal likely contribute to SOA formation in slightly acidic media and hydration and polymerization of methylglyoxal in the atmospheric aerosol-phase are dependent on the hygroscopicity, rather than the acidity of the aerosols. Because a low-pressure fast flow reactor was used in the present work, the sulfuric acid concentrations used were rather high. Further experimental studies are needed to confirm the observed trend of increasing uptake of methylglyoxal with decreasing acidity to the low acidity range.

Acknowledgments

Literature Cited

(1) Carey, F. A.; Sundberg, R. J. *Advanced Organic Chemistry: Part A Structure and Mechanisms,* 4th ed.; Plenum Press: New York, 2000.

(2) Barton, D. in *Comprehensive Organic Chemistry: The Synthesis and Reactions of Organic Compounds*; Ollis, W. D., Ed.; Pergamon Press: New York, 1979; pp 960–1013.

(3) Jang, M.; Czoschke, N. M.; Lee, S.; Kamens, R. M. Heterogeneous atmospheric aerosol production by acid-catalyzed particle-phase reactions. *Science* **2002**, *298*, 814–817.

(4) Kalberer, M.; Poulsen, D.; Sax, M.; Steinbacher, M.; Dommen, J.; Prevot, A. S. H.; Fisseha, R.; Weingartner, E.; Frankevich, V.; Zenobi, R.; Baltensperger, U. Identification of polymers as major components of atmospheric organic aerosols. *Science* **2004**, *303*, 1659–1662.

(5) Andreae, M. O.; Crutzen, P. J. Atmospheric aerosols: Biogeochemical sources and role in atmospheric chemistry. *Science* **1997**, *276*, 1052–1058.

(6) Zhang, R.; Suh, I.; Zhao, J.; Zhang, D.; Fortner, E. C.; Tie, X.; Molina, L. T.; Molina, M. J. Atmospheric new particle formation enhanced by organic acids. *Science* **2004**, *304*, 1487–1490.

(7) Fan, J.; Zhang, R. Atmospheric oxidation mechanism of p-Xylene: A density functional theory study. *J. Phys. Chem. A* **2006**, *110*, 7728–7737.

(8) Suh, I.; Zhang, R.; Molina, L. T.; Molina, M. J. Oxidation mechanism of aromatic peroxy and bicyclic radicals from OH-toluene reactions. *J. Am. Chem. Soc.* **2003**, *125*, 12655–12665.

(9) Zhao, J.; Zhang, R.; Misawa, K.; Shibuya, K. Experimental product study of the OH-initiated oxidation of m-xylene. *J. Photochem. Photobiol. A* **2005**, *176*, 199–207.

(10) Grosjean, E.; Grosjean, D.; Fraser, M. P.; Cass, G. R. Air quality model evaluation data for organics .2. C-1-C-14 carbonyls in Los Angeles air. *Environ. Sci. Technol.* **1996**, *30*, 2687–2703.

(11) Chen, Y.; Wang, W.; Zhu, L. Wavelength-dependent photolysis of methylglyoxal in the 290–440 nm region. *J. Phys. Chem. A* **2000**, *104*, 11126–11131.

(12) Zhao, J.; Levitt, N. P.; Zhang, R. Heterogeneous chemistry of octanal and 2,4-hexadienal with sulfuric acid. *Geophys. Res. Lett.* **2005**, *32*, L09802, doi:10.1029/ 2004GL022200.

(13) Zhang, R.; Wooldridge, P. J.; Abbatt, J. P. D.; Molina, M. J. Physical chemistry of the sulfuric acid/water binary system at low temperatures: stratospheric implications. *J. Phys. Chem.* **1993**, *97*, 7351–7358.

(14) Zhang, R.; Wooldridge, P. J.; Molina, M. J. Vapor pressure measurements for sulfuric acid/nitric acid/water and sulfuric acid/hydrochloric acid/water systems: incorporation of stratospheric acids into background sulfate aerosols. *J. Phys. Chem.* **1993**, *97*, 8541–8548.

(15) Gurnick, M.; Chaiken, J.; Benson, T.; McDonald, J. D. Vibrational and rotational spectroscopy of the first electronically allowed transition of α–dicarbonyls. *J. Chem. Phys.* **1981**, *74*, 99–105.

(16) Mackay, D.; Bobra, A.; Chan, D. W.; Shiu, W. Y. Vapor-pressure correlations for low-volatility environmental chemicals. *Environ. Sci. Technol.* **1982**, *16*, 645–649.

(17) Schwarzenbach, R. P.; Gschwend, P. M.; Imboden, D. M. *Environmental Organic Chemistry;* Wiley: New York, 1993.

(18) Zhao, L.; Ni, N.; Yalkowsky, S. H. A modification of Trouton's rule by simple molecular parameters for hydrocarbon compounds. *Ind. Eng. Chem. Res.* **1999**, *38*, 324–327.

(19) Zhao, L.; Ni, N.; Yalkowsky, S. H. Predicting the entropy of boiling for organic compounds. *J. Chem. Inf. Comput. Sci.* **1999**, *39*, 1112–1116.

(20) *Handbook of Chemistry and Physics*, 83rd ed.; Lide, D. R., Ed.; CRC press: New York, 2002–2003.

(21) Fortner, E. C.; Zhao, J.; Zhang, R. Development of ion drift-chemical ionization mass spectrometry. *Anal. Chem.* **2004**, *76*, 5436–5440.

(22) Zhao, J.; Fortner, E. C.; Zhang, R. Quantification of hydroxy-carbonyls from OH-isoprene reactions. *J. Am. Chem. Soc.* **2004**, *126*, 2686–2687.

(23) Timonen, R. S.; Chu, L. T.; Leu, M. T.; Keyser, L. F. Heterogeneous reaction of ClONO2(g) + NaCl(s) .fwdarw. Cl2(g) + NaNO3(s). *J. Phys. Chem.* **1994**, *98*, 9509–9517.

(24) Jayne, J. T.; Worsnop, D. R.; Kolb, C. E.; Swartz, E.; Davidovits, P. Uptake of Gas-Phase Formaldehyde by Aqueous Acid Surfaces. *J. Phys. Chem.* **1996**, *100*, 8015–8022.

(25) Zhang, D.; Zhang, R. Laboratory investigation of heterogeneous interaction of sulfuric acid with soot. *Environ. Sci. Technol.* **2005**, *39*, 5722–5728.

(26) Klassen, J. K.; Lynton, J.; Golden, D. M.; Williams, L. R. Solubility of acetone in low-temperature (210–240 K) sulfuric acid solutions. *J. Geophy. Res.* **1999**, *104*, 26355–26361.

(27) Betterton, E. A.; Hoffmann, M. R. Henry's law constants of some environmentally important aldehydes. *Environ. Sci. Technol.* **1988**, *22*, 1415–1418.

(28) Liggio, J.; Li, S. M.; McLaren, R. Reactive uptake of glyoxal by particulate matter. *J. Geophys. Res.* **2005**, *110*, D10304, doi:10.1029/2004JD005113.

(29) Nemet, I.; Drazen, V. T.; Varga-Defterdarovic, L. Spectroscopic studies of methylglyoxal in water and dimethylsulfoxide. *Bioorg. Chem.* **2004**, *32*, 560–570.

(30) Whipple, E. B. Structure of glyoxal in water. *J. Am. Chem. Soc.* **1970**, *92*, 7183–7186.

(31) Garner, H. K.; Lucas, H. J. Preparation and hydrolysis of some acetals and esters of D(-)-2,3-butanediol. *J. Am. Chem. Soc.* **1950**, *72*, 5497–5501.

(32) Deno, N. C.; Newman, M. S. Mechanism of sulfation of alcohols. *J. Am. Chem. Soc.* **1950**, *72*, 3852−3856.

(33) Clark, D. J.; Williams, G. Esterification by sulphuric acid .2. alcohol. *J. Chem. Soc.* **1957**, 4218−4221.

(34) Liggio, J.; Li, S. M.; McLaren, R. Heterogeneous reactions of glyoxal on particulate matter: Identification of acetals and sulfate esters. *Environ. Sci. Technol.* **2005**, *39*, 1532−1541.

(35) Iraci, L. T.; Tolbert, M. A. Heterogeneous interaction of formaldehyde with cold sulfuric acid: Implications for the upper troposphere and lower stratosphere. *J. Geophys. Res.* **1997**, *102*, 16099−16107.

(36) Kroll, J. H.; Ng, N. L.; Murphy, S. M.; Varubangkul, V.; Flagan, R. C.; Seinfeld, J. H. Chamber studies of secondary organic aerosol growth by reactive uptake of simple carbonyl compounds. *J. Geophys. Res.* **2005**, *110*, D23207, doi:10.1029/2005JD006004.